

Rheological and physical characterization of PEDOT: PSS/graphene oxide nanocomposites for perovskite solar cells

Antonella Giuri, Sofia Masi, Silvia Colella, Andrea Listorti, Aurora Rizzo, Alessandro Kotuvn, Simone Dell'Elce, Andrea Liscio, Carola Esposito Corcione

A. Giuri, Dr. C. Esposito Corcione

Dipartimento di Ingegneria dell'Innovazione, Università del Salento, via per Monteroni, km 1, 73100, Lecce, Italy

Dr. S. Masi, Dr. A. Rizzo

Istituto di Nanotecnologia CNR-Nanotec, Polo di Nanotecnologia c/o Campus Ecotekne, via Monteroni, 73100 Lecce, Italy

Dr. S. Colella, Dr. A. Listorti

Dipartimento di Matematica e Fisica "E. De Giorgi", Università del Salento, Via Arnesano snc, 73100 Lecce, Italy

A. Kotuvn, S. Dell'Elce, Dr. A. Liscio

Istituto per la Sintesi Organica e la Fotoreattività CNR-ISOF, via Gobetti 101, 40120, Bologna, Italy

Rheological and physical characterization of PEDOT: PSS/graphene oxide nanocomposites for perovskite solar cells

Antonella Giuri¹, Sofia Masi², Silvia Colella^{2,3}, Andrea Listorti^{2,3}, Aurora Rizzo², Alessandro Kotuvn⁴, Simone Dell'Elce⁴, Andrea Liscio⁴, Carola Esposito Corcione¹

¹ Dipartimento di Ingegneria dell'Innovazione, Università del Salento, via per Monteroni, km 1, 73100, Lecce, Italy

² Istituto di Nanotecnologia CNR-Nanotec, Polo di Nanotecnologia c/o Campus Ecotekne, via Monteroni, 73100 Lecce, Italy

³ Dipartimento di Matematica e Fisica "E. De Giorgi", Università del Salento, Via Arnesano snc, 73100 Lecce, Italy

⁴ Istituto per la Sintesi Organica e la Fotoreattività CNR-ISOF, via Gobetti 101, 40120, Bologna, Italy

ABSTRACT

In this work, the influence of graphene oxide (GO) doped Poly(3,4 ethylenedioxythiophene):poly(styrenesulfonate)(PEDOT:PSS) thin nanocomposite on an indium–tin-oxide (ITO) anode, as hole transport layer (HTL) in perovskite solar cells, was investigated. Different concentrations of GO were added into the PEDOT:PSS in order to enhance its conductivity. In particular, the influence of GO content on the rheological and thermal properties of Poly(3,4-ethylenedioxythiophene):poly(styrenesulfonate) (PEDOT:PSS)/GO nanocomposites was initially examined. The GO filler was prepared by using modified Hummers method and dispersed into PEDOT:PSS in different quantity (ranging from 0.05 to 0.25 %wt/wt). The obtained nanocomposite solutions were analyzed by rheological characterizations in order to evaluate the influence of the GO filler on the viscosity of the PEDOT:PSS matrix. The wettability of solutions was evaluated by Contact Angle (CA) measurements. The quality of GO dispersion into the polymer matrix was studied using Scanning electron microscopy (SEM) and X-ray diffraction (XRD). Thermal characterizations (DSC and TGA) were, finally, applied on nanocomposite films in order to evaluate thermal stability of the films as well as to indirectly comprehend the GO influence on PEDOT:PSS-water links.

INTRODUCTION

Since the discovery of conductive polyacetylene in 1978 [1-3], conductive polymers have attracted the attention worldwide because they combine the properties of metals and polymers [4]. However, application and processability of the conducting polymers are not always easy to balance [5].

Poly(3,4-ethylenedioxythiophene):poly(styrenesulfonate) (PEDOT:PSS) is one of the most successful conjugated polymers being used commercially as charge extractor since they were synthesized in the late 1980s [5]. PEDOT:PSS films can be readily deposited on substrates by the conventional solution processing techniques [6,7]. PEDOT:PSS is a polyelectrolyte with the hydrophobic PEDOT and hydrophilic PSS, among which a Coulombic interaction exists: PSS of PSS anions' segments attached with PEDOT are screened by the positive charges on PEDOT. Moreover, the PSS segments form blobs for preventing the contact of PEDOT from water in order to reduce the interactions between PEDOT and water. The blobs have a core/shell structure with PEDOT in the core and PSS in the shell [4,8].

To date, the solid polyelectrolyte PEDOT-PSS was the most common organic charge extraction layer used in polymer solar cells. It allows efficient charge extraction and transport, but suffers important drawbacks related to the stability of the PEDOT:PSS itself [9-11]. Aiming at enhancing the electrical conductivity and the stability of polymeric matrices for photovoltaic applications, the doping of PEDOT:PSS by graphene based filler has attracted great attention and has shown interesting results [12-16].

Graphene, a two-dimensional carbon layer, shows, in fact, interesting thermal, elastic, optical, electrical, and mechanical properties. Despite the extraordinary properties, the graphene production, including chemical vapor deposition (CVD), mechanical exfoliation, epitaxial growth [17], requires expensive, complex and not often compatible with upscaling processes. An alternative and promising approach to produce large amount of solution processable graphene is the reduction of graphene oxide (GO) dispersions. Prepared by modified Hummer's method [18,19], GO is a single layer graphene-based material presenting different chemical functional groups such as oxygen

epoxides (bridging oxygen atoms), carbonyls (C=O), hydroxyls (-OH) and phenols. Forming stable solutions in water, GO is high-processable, flexible, and low-cost material, having remarkable potential applications for consumer electronics. The disrupted sp² conjugation of the graphene lattice leads to a deterioration of conductivity, but its residual sp² clusters can still allow hole transportation to occur via hopping [20]. The electrical conductivity can be recovered by reducing GO, removing the oxygen-contained in the functional groups. Thermal and chemical approaches are typically used to reduce GO, exploiting high temperature (up to 900°C) or toxic chemical agent (i.e. hydrazine). Green approaches such as UV irradiation [21-23] or glucose [24] as reduction agents, are recently presented showing interesting results in term of reduction efficiency [15-17,21,23,25]. We recently demonstrated the improvement of the performance of photovoltaic devices by blending PEDOT:PSS and reduced graphene oxide (RGO) as thin film electrode [15,16]. The change of the surface wettability improves the homogeneity of the upper PEDOT:PSS layer while the presence of reduced GO sheets restores and improves the electrical conductivity of the film. [15,16].

The understanding of the role of GO into the PEDOT:PSS matrix is crucial to simplify the process of the film production and as well as to improve the performance of the device. In this work, we report a detailed investigation of the influence of GO on the rheological, morphological and thermal properties of the composite.

Experimental

Materials

PEDOT:PSS aqueous solution (Clevios PVP AI4083) was purchased from Heraeus with a PEDOT:PSS concentration of 1.3 %w/w (weight ratio of PSS to PEDOT = 6).

GO was prepared using modified Hummers method [18] yielding GO flakes with maximum lateral size of 100 μm [19].

GO/PEDOT:PSS nanocomposite preparation

The dispersion of GO into PEDOT:PSS was obtained by the solvent swelling method [15,16,26]. GO was added into PEDOT:PSS and the blend was magnetically stirred for 90' and sonicated for 15' at room temperature (RT). The influence of each component was studied by preparing different concentrations of GO/PEDOT:PSS dispersions:(0.05, 0.15, 0.25 %wt/wt (Table 1). The blend was deposited at RT in air on different substrates in accordance with the type of characterization performed.

Experimental techniques

The rheological characterization of the all formulations produced was carried out in a strain controlled rheometer (Ares TA Instrument). Viscosity was measured at 20.5 °C using a parallel plate geometry (radius=12.5 mm) in steady state mode with a shear rate ranging from 0.05 to 600 s⁻¹. A pre-shear experiment was run prior to each test, and the rheological experiments were repeated at least three times for checking the repeatability of results. At the end of the rheological characterization, an appropriate theoretical equation was identified for each system in order to fit the experimental data.

GO/PEDOT:PSS dispersions were drop casted on a glass substrate and analyzed, after water evaporation, by XRD in order to evaluate the quality of GO dispersion into PEDOT:PSS. The XRD (Rigaku, Tokyo, Japan) pattern was obtained with CuK α radiation ($\lambda=1.5418 \text{ \AA}$) in the step scanning mode recorded in the 2θ range of 5°–50°, with a step size of 0.02° and step duration of 0.5 s.

GO/PEDOT:PSS solutions were spin coated on ITO substrates at 2500 rpm for 60'' and annealed at 140°C for 1h in N₂ atmosphere in order to analyze the morphology of the films obtained by SEM, and in particular to evaluate the quality of various GO dispersions into PEDOT:PSS.

SEM micrographs were obtained using Carl Zeiss Auriga40 Crossbeam instrument, in high vacuum

and high-resolution acquisition mode, equipped with Gemini column and an integrated high efficiency in-lens detector. The applied acceleration voltage was 2 or 5 kV.

The thermal stability of pristine PEDOT:PSS and GO/PEDOT:PSS was investigated by thermogravimetric analyses, carried out on a TGA/DSC 1 manufactured by Mettler Toledo, under a nitrogen atmosphere created by fluxing 50 ml/min of N₂ from 20°C to 600°C at the heating rate of 10°C/min. About 5 mg of sample was put into alumina pan for the test after air drying for 96 hours samples drop casted on cleaned silicone sheet [27]. The results obtained from TGA in the range of 20-160°C were combined with the analysis by a differential scanning calorimeter (DSC Mettler Toledo 622) in order to comprehend the reaction that occurs in all the systems. About 5 mg of dried samples for 96 hours on silicone sheet were put into aluminum flat disks and heated from 20 up to 160°C at 10°C/min under nitrogen atmosphere flow at 80 mL/min. After free cooling up to room temperature, a second heating scan was performed.

The wettability of PEDOT:PSS and GO/PEDOT:PSS blends on ITO substrates was evaluated by contact angle (CA) measurements with a First Ten Angstroms FTA1000 Quick start instrument.

The nanocomposite dispersions were spin coated on a quartz substrate and analyzed by UV–visible spectrophotometer (Varian Cary 500) after thermal annealing in order to evaluate the influence of GO concentration on film absorption. The Ultraviolet–visible absorption spectra were recorded in the 200–800 nm wavelength range at room temperature.

Results and discussion

The viscosity of neat PEDOT:PSS as a function of the shear rate (ranging from 0.05 to 600 s⁻¹) was compared with that of PEDOT:PSS filled with different GO contents (0.05, 0.15 and 0.25 %wt/wt) and reported in Figure 1(a). A pseudo-plastic behavior was evidenced for each mixture investigated. After adding GO, the viscosity of the PEDOT:PSS increases, probably due to the interaction between the functional groups of GO and PEDOT:PSS. In order to estimate the value of the viscosity reached during the film deposition (by spin coating at 3000 rpm), the shear rate reached

during the spin coating process was calculated by using the following equation:

$$\dot{\gamma} = \frac{v}{h}$$

(1)

Where, v is the tangential velocity (equal to the product of angular spin coating velocity and the radius of rheometer plate) and h is the sample thickness (i.e. the distance between the plates among which there is the solution).

The shear rate calculated, starting from eq. (1), is 9817.5 s^{-1} , which is out of the measurement range of the available rheometer (i.e. 600 s^{-1}). For this reason, proper theoretical models were applied to fit the experimental data, reported in Figure 1(a). In details, Cross [28] proposed a model allowing to predict the plateau values for lower and upper Newtonian viscosities, indicated as η_0 and η_∞ , respectively:

$$\eta = \eta_\infty + \frac{\eta_0 - \eta_\infty}{1 + (\tau \dot{\gamma})^m} \quad (2)$$

where, τ and m are model parameters and $\dot{\gamma}$ the shear rate.

In particular, τ corresponds to the reciprocal of the shear rate at which the calculated value of η equals η_0 , while the parameter m is related to the power law index, n , by the expression: $m=1-n$.

The values of the parameters in eq. (2), calculated by a non linear fitting of the experimental data shown in Figure 1(a), are reported in Table 2. At very low shear rates, the viscosity of GO/PEDOT mixtures is considerably higher than that of pure PEDOT:PSS, as already pointed out. In particular, GO_{0.25}PEDOT formulation possesses the highest viscosity. At higher shear rate values (i.e., η_∞), the viscosity of the mixtures is also higher than that of pure PEDOT:PSS, especially in the presence of 0.15 and 0.25 %wt of GO. The values of the parameter m , calculated for the mixtures containing GO, are very similar and different from that of neat PEDOT:PSS, as witnessed by their rheological

curves. On the other hand, the values of τ increases by increasing the content of GO, indicating that the pseudo-plastic behavior starts at lower shear rate values for the nanocomposite mixtures.

The experimental data of Figure 1 (a) was fitted (at high shear rate), by using Batchelor equation [29], obtained from the correction of the classical Einstein model, in order to take into account the effect of more concentrated suspensions of particles ($\phi > 0.02$) [30-32]:

$$\eta_r = \frac{\eta_\infty}{\eta_{\infty S}} = 1 + k_1 * \phi + k_2 * \phi^2 \quad (3)$$

where, η_∞ is the viscosity of the GO/PEDOT solutions at high shear rate, and $\eta_{\infty S}$ the viscosity of the suspending medium PEDOT:PSS at high shear rate.

The volume fraction (ϕ) of GO into GO/PEDOT solutions was calculated by applying the rule of mixtures starting from the density of the mixtures (Table 1).

Referring to the physical significance of the k_1 and k_2 parameters introduced in Eq. (3), k_1 takes into account the shape of the particles in suspension. Guth found that in the case of non-spherical particles, k_1 depends on the aspect ratio [30,31,33], p , according to following equation:

$$k_1 = \frac{p}{2 \ln(2p) - 3} + 2 \quad (4)$$

k_2 was first introduced by Batchelor in order to consider the increase in the viscosity taking place in more concentrated suspensions.

The theoretical predictions obtained by applying this model were in good agreement with the experimental rheological data of Figure 1(a), as shown in Figure 1(b). They also allowed determining the following numerical values of the parameters k_1 and k_2 : 30.2 and 119.6 respectively. The value of the aspect ratio, p , obtained from Eq. (3) and (4), irrespective of the filler concentration, is 270, evidencing that a not complete exfoliation of GO was obtained in the polymer matrix.

The rheological characterization shows that a good dispersion of the GO filler into PEDOT:PSS was obtained by the solvent swelling method, used in this work. After adding GO to the PEDOT:PSS, the dimension of the filler was still nanometric, also at high GO concentration, and the viscosity of the nanocomposite solutions has reached values still suitable to the film processing by spin coating, which is the standard deposition method used for PEDOT:PSS for photovoltaic application.

In order to confirm the good quality of the GO dispersion, XRD measurements, were carried out on PEDOT:PSS and nanocomposite films, drop casted on a glass substrate.

The X-ray diffraction patterns of the GO filler, reported in our previous papers [16,34], evidence the presence of the characteristic (001) diffraction peak of GO at $2\theta=11.12^\circ$ (black vertical line in Figure 2), corresponding to an interlayer distance of about 0.80 nm. When GO was incorporated in PEDOT:PSS, the 001 reflection disappeared, confirming the complete loss of the crystalline order perpendicular to the graphitic planes, probably due to the good dispersion of the GO sheet in the polymer matrix, with the intercalation of the polymer chain between GO sheet and the consequent complete GO exfoliation. However, in the presence of 0.25% wt. of GO, a slight band appears at low degree, attributed to a possible aggregation of GO filler, due to the higher GO concentration.

This latter behavior was also confirmed by SEM analysis performed on the films deposited by spin coating on ITO substrate. GO_{0.05}PEDOT solution appears as a continuous film with some GO aggregates, meanwhile by increasing GO content up to 0.25% wt., the presence of the aggregates increases, which can be seen in Figure 3. By using the software of image analysis, Image J, the average diameter of the fillers, calculated from SEM images, was equal to 24 and 35 for 0.05 and 0.25% of GO content, respectively. Higher GO concentration determines the presence of higher GO aggregates, as shown by the previous characterization. However, both XRD and SEM analyses show good and homogeneous GO dispersion into PEDOT:PSS matrix, also at lower GO concentration, confirming that the method used in this work was appropriate for the nanocomposite preparation.

Before the thermal annealing, thermal analysis (DSC/TGA) was carried out on the films in order to better understand the influence of the several concentrations of GO on thermal stability of neat PEDOT:PSS.

DSC analysis shows that all the films exhibit broad endothermic peak between 20 and 160 °C, during the first annealing (Figure 4(a)), which disappears during the second annealing. This indicates that the film releases water during the heating process, as observed by Zhou et al. [27], and is also confirmed by the first weight loss step of TGA curves of the films from 20°C to about 155°C reported in Figure 4(b) [27,35]. The TGA curves of Figure 4(b) evidence a weight loss of 22.7% for the neat PEDOT:PSS film, which slightly decreases by adding GO to about 18.9%.

Combining DSC and TGA results together provides more refined information about the water loss and the energy associated to their weight loss, allowing to calculate the characteristic energy for dehydration by using the following equation:

$$E = M \left(\frac{\Delta Q}{\Delta W} \right) \quad (5)$$

where, M is the water molecular weight (18 g mol⁻¹), ΔQ is the amount of the heat absorbed during the dehydration, estimated from DSC, and ΔW is the weight loss of water estimated from TGA. Both thermal analysis were performed in the temperature range between 20 and 155 °C.

The characteristic dehydration energy calculated for all the films is in the range of the energy of moderate hydrogen bonds (10 to 60 kJ mol⁻¹). This suggests that the water molecules are hydrogen-bonded with PSS chains in PEDOT:PSS [27] and probably with OH groups in the samples containing GO. However, the characteristic dehydration energy for the PEDOT:PSS decreases from 39 to 33 kJ mol⁻¹ by adding 0.05% of GO, while it increases up to 54 and 41 kJ in the presence of 0.15 and 0.25% of GO respectively, showing a different interaction with water molecules influenced by the presence of the doping element in the PEDOT:PSS.

The exothermic peak, at around 190°C, which appears in the DSC thermogram of the nanocomposite, in the presence of 0.15 and 0.25% wt of GO, can be certainly attributed to the

removal of labile oxygen functional groups, consequently to the thermal reduction of GO dispersed in the polymer matrix [36]. This peak was not observed in the presence of 0.05% of GO, probably because the oxygen content groups of GO, lost during the thermal treatment, were very low to be sensed by the instrument. This was confirmed by TGA analysis, indeed it evidences a second weight loss of about 8% from 155 to 250°C for the samples containing 0.15 and 0.25% of GO, which is not observed for pristine PEDOT:PSS and PEDOT:PSS with 0.05% of GO.

The third weight loss, observed by TGA analysis, from 250°C to about 600°C, was due to oxidizing decomposition of the skeletal PEDOT and/or PSS backbone chain structure [35]. In particular, at around 250°C, the PSS sulfonate group fragmentation occurs and over 350°C, the carbon oxidation is evident [37]. As reported in Table 3, the thermal degradation of PEDOT:PSS became at about 268°C up to 510°C and causes a weight loss of 36%. By adding GO, the onset point was delayed, in particular in the presence of 0.15 and 0.25%, and the residue was increased, showing that GO influences the thermal stability of PEDOT:PSS. In particular, the possible reduction of GO, caused by temperature, has the potentiality to positively influence the stability of the film by increasing it. This is an important result for the purpose of photovoltaic application.

All the films are thermally stable at 140°C, so no degradation occurs during annealing treatment. Both the characterizations confirmed that the nanocomposite films were appropriate for the selected application, since the presence of the filler does not affect the temperature of film processing and their thermal stability, rather than increasing it. Therefore, the processing parameters used for the PEDOT:PSS deposition can be used to deposit the nanocomposite films.

The influence of GO doping on the wettability of PEDOT:PSS on ITO was evaluated by contact angle measurements (Figure 5). The addition of GO into PEDOT:PSS reduces the contact angle of PEDOT:PSS based solutions on ITO substrate from $93.6^\circ \pm 6.2$ to $81.5^\circ \pm 0.6$ (Figure 5(a)), ensuring better coverage of substrate. The solution adhesion, in fact, became higher by increasing GO concentration in the PEDOT:PSS, suggesting that the presence of GO improves the interfacial adhesion than the lower substrate compatibility, basic factor to obtain a good layer in a photovoltaic

application.

In addition the UV-vis absorption measurements, reported in Figure 6, show that the spectra of PEDOT:PSS does not change by adding GO, after annealing at 140°C.

CONCLUSION

The effect of an experimental graphene oxide (GO), prepared by a modified Hummers method, on the thermal and physical properties of Poly(3,4 ethylenedioxythiophene):poly(styrenesulfonate)(PEDOT:PSS), applied on an indium–tin-oxide (ITO) anode, as hole transport layer (HTL) in perovskite solar cells, was investigated as a function of the GO concentration. The viscosity of the GO/PEDOT:PSS mixtures increases by increasing GO content, still remaining appropriate for the spin coating process, conventionally used for the PEDOT:PSS deposition in the specific application and showing, in turn, a good dispersion of the GO filler into the conductive matrix. This latter behavior was also confirmed by XRD analysis, since the GO/PEDOT:PSS pattern evidenced the disappearance of the typical XRD 001 reflection peak of GO, suggesting the complete loss of the crystalline order perpendicular to the graphitic planes. However, due to a possible aggregation of the GO filler, the highest concentration of GO (i.e. 0.25% wt.) showed a slight band at low degree. This latter result was also evident from SEM analysis, performed on the films deposited by spin coating on ITO substrate. The thermal analysis, performed by TGA and DSC, evidenced a possible reduction of GO, caused by the increased temperature. This is an important result for the purpose of photovoltaic application, since the reduction of GO could improve the stability of the composite film. In addition, the presence of GO in PEDOT:PSS matrix guarantees better coverage of the substrate, as evidenced by the reduction of the contact angle of the PEDOT:PSS based solutions on ITO substrate from about 94° to about 81°, which allows better adhesion of the solution, by increasing GO concentration in the PEDOT:PSS, remaining unchanged the UV vis absorption capability.

- [1] T. A. Skotheim, Marcel Dekker (1986).
- [2] J. R. Reynolds, T. A. Skotheim, and R. L. Elsenbaumer, *Handbook of conducting polymers* Marcel Dekker (1998).
- [3] T. A. Skotheim and J. Reynolds, *Handbook of Conducting Polymers, 2 Volume Set*, CRC press (2007).
- [4] J. Ouyang, *Displays* **34**, 423 (2013).
- [5] S. Jönsson, J. Birgersson, X. Crispin, G. Greczynski, W. Osikowicz, A. D. Van Der Gon, W. R. Salaneck, and M. Fahlman, *Synthetic Met.* **139**, 1 (2003).
- [6] L. Groenendaal, F. Jonas, D. Freitag, H. Pielartzik, and J. R. Reynolds, *Adv. Mater.* **12**, 481 (2000).
- [7] Y. Cao, G. Yu, C. Zhang, R. Menon, and A. Heeger, *Synthetic Met.* **87**, 171 (1997).
- [8] U. Lang, E. Müller, N. Naujoks, and J. Dual, *Adv. Funct. Mater.* **19**, 1215 (2009).
- [9] A. Mei *et al.*, *Science* **345**, 295 (2014).
- [10] N. J. Jeon, J. H. Noh, Y. C. Kim, W. S. Yang, S. Ryu, and S. I. Seok, *Nat. mater.* **13**, 897 (2014).
- [11] N. J. Jeon, J. H. Noh, W. S. Yang, Y. C. Kim, S. Ryu, J. Seo, and S. I. Seok, *Nature* **517**, 476 (2015).
- [12] T. Liu, D. Kim, H. Han, A. R. bin Mohd Yusoff, and J. Jang, *Nanoscale* **7**, 10708 (2015).
- [13] A. Fallahi, M. Alahbakhshi, E. Mohajerani, F. Afshar Taromi, A. R. Mohebbi, and M. Shahinpoor, *J. Phys. Chem. C* **119**, 13144 (2015).
- [14] S. I. Ahn, K. Kim, J. R. Jung, K. Y. Kang, S. M. Lee, J. Y. Han, and K. C. Choi, *Chem. Phys. Lett.* **625**, 36 (2015).
- [15] A. Giuri *et al.*, *IEEE Transactions on Nanotechnology* **PP** (2016).
- [16] A. Giuri *et al.*, *Adv. Funct. Mater.* **26**, 6985 (2016).
- [17] S. Pei and H.-M. Cheng, *Carbon* **50**, 3210 (2012).
- [18] M. Hirata, T. Gotou, S. Horiuchi, M. Fujiwara, and M. Ohba, *Carbon* **42**, 2929 (2004).

- [19] F. Perrozzi *et al.*, *J. Phys. Chem. C* **117**, 620 (2012).
- [20] H. S. Dehsari, E. K. Shalamzari, J. N. Gavgani, F. A. Taromi, and S. Ghanbary, *RSC Adv.* **4**, 55067 (2014).
- [21] Y. H. Ding, P. Zhang, Q. Zhuo, H. M. Ren, Z. M. Yang, and Y. Jiang, *Nanotechnology* **22**, 215601 (2011).
- [22] A. Giuri *et al.*, *Sci. Adv. Mater.* **7**, 2445 (2015).
- [23] S. Rella, A. Giuri, C. E. Corcione, M. R. Acocella, S. Colella, G. Guerra, A. Listorti, A. Rizzo, and C. Malitesta, *Vacuum* **119**, 159 (2015).
- [24] S. G. Chengzhou Zhu, Youxing Fang, and Shaojun Dong, *ACS Nano* **4**, 2429 (2010).
- [25] S. Stankovich, D. A. Dikin, R. D. Piner, K. A. Kohlhaas, A. Kleinhammes, Y. Jia, Y. Wu, S. T. Nguyen, and R. S. Ruoff, *Carbon* **45**, 1558 (2007).
- [26] M. Mauro, M. R. Acocella, C. E. Corcione, A. Maffezzoli, and G. Guerra, *Polymer* **55**, 5612 (2014).
- [27] J. Zhou, D. H. Anjum, L. Chen, X. Xu, I. A. Ventura, L. Jiang, and G. Lubineau, *J. Mater. Chem. C* **2**, 9903 (2014).
- [28] M. M. Cross, *J. Colloid Sci.* **20**, 417 (1965).
- [29] G. Batchelor, *J. Fluid Mech.* **83**, 97 (1977).
- [30] C. E. Corcione, F. Freuli, and A. Maffezzoli, *Polym. Eng. & Sci.* **53**, 531 (2013).
- [31] C. Esposito Corcione, G. Mensitieri, and A. Maffezzoli, *Polym. Eng. Sci.* **49**, 1708 (2009).
- [32] A. Einstein, *Phys* **19**, 289 (1906).
- [33] C. E. Corcione, A. Cavallo, E. Pesce, A. Greco, and A. Maffezzoli, *Polym. Eng. Sci.* **51**, 1280 (2011).
- [34] A. Giuri, S. Colella, A. Listorti, A. Rizzo, and C. E. Corcione, in *VIII INTERNATIONAL CONFERENCE ON "TIMES OF POLYMERS AND COMPOSITES": From Aerospace to Nanotechnology* (AIP Publishing, 2016), p. 020115.

- [35] Y. Xu, Y. Wang, J. Liang, Y. Huang, Y. Ma, X. Wan, and Y. Chen, *Nano Research* **2**, 343 (2009).
- [36] S. Park, J. An, J. R. Potts, A. Velamakanni, S. Murali, and R. S. Ruoff, *Carbon* **49**, 3019 (2011).
- [37] A. Elschner, S. Kirchmeyer, W. Lovenich, U. Merker, and K. Reuter, *PEDOT: principles and applications of an intrinsically conductive polymer*, CRC Press (2010).

Figure 1. (a) Rheological behavior of unfilled PEDOT:PSS compared with those of PEDOT:PSS containing 0.05, 0.15 and 0.25 %wt of GO; (b) Comparison between the experimental relative viscosity and the prediction from Batchelor equation (Eq. 2) of PEDOT:PSS solutions containing 0.05, 0.15 and 0.25% wt of GO

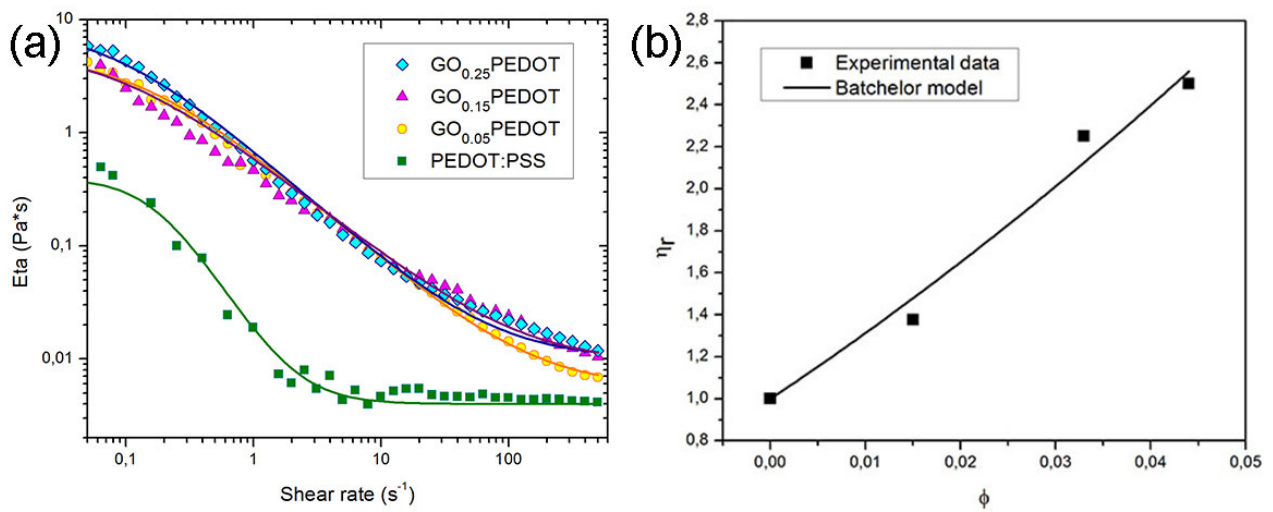


Figure 2. XRD of unfilled PEDOT:PSS compared with those of PEDOT:PSS containing 0.05, 0.15 and 0.25 %wt of GO dropped on glass substrate

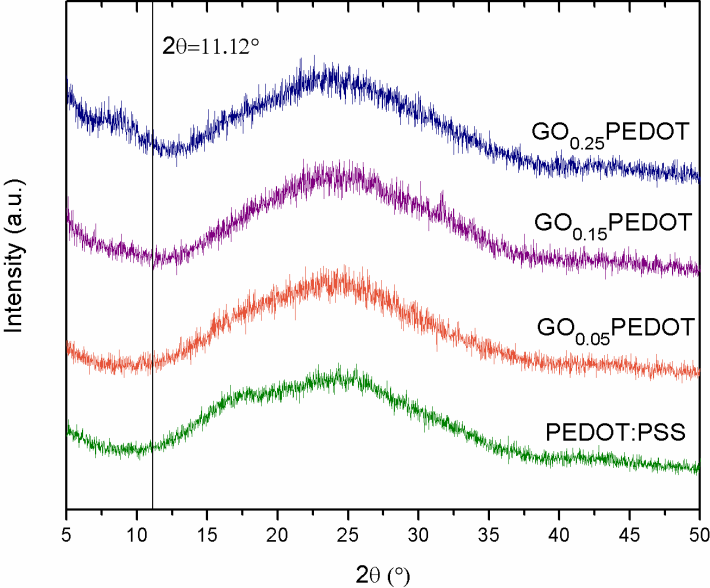


Figure 3. SEM of $\text{GO}_{0.05}\text{PEDOT}$ (left) and $\text{GO}_{0.25}\text{PEDOT}$ (right) nanocomposite films, magnification in the insert

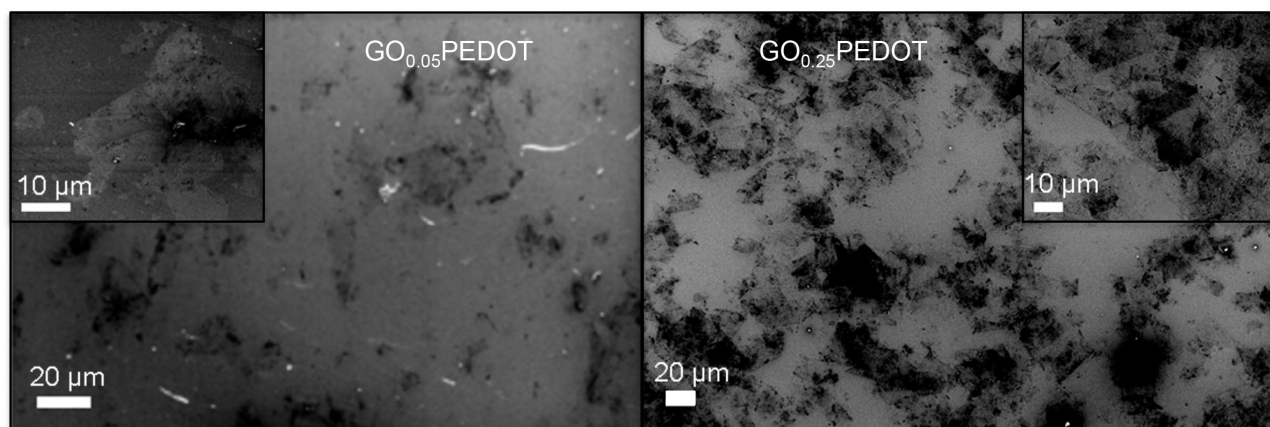


Figure 4. DSC (a) and TGA (b) curves of the PEDOT:PSS, GO_{0.05}PEDOT, GO_{0.15}PEDOT, GO_{0.25}PEDOT films.

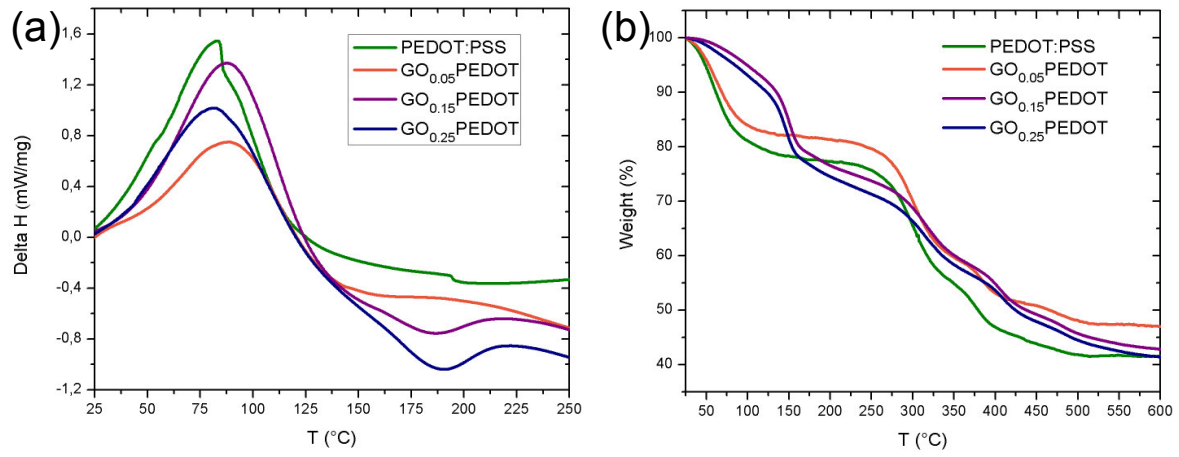


Figure 5. Contact angle values (a) and drops (b) of PEDOT:PSS and nanocomposite solutions on ITO

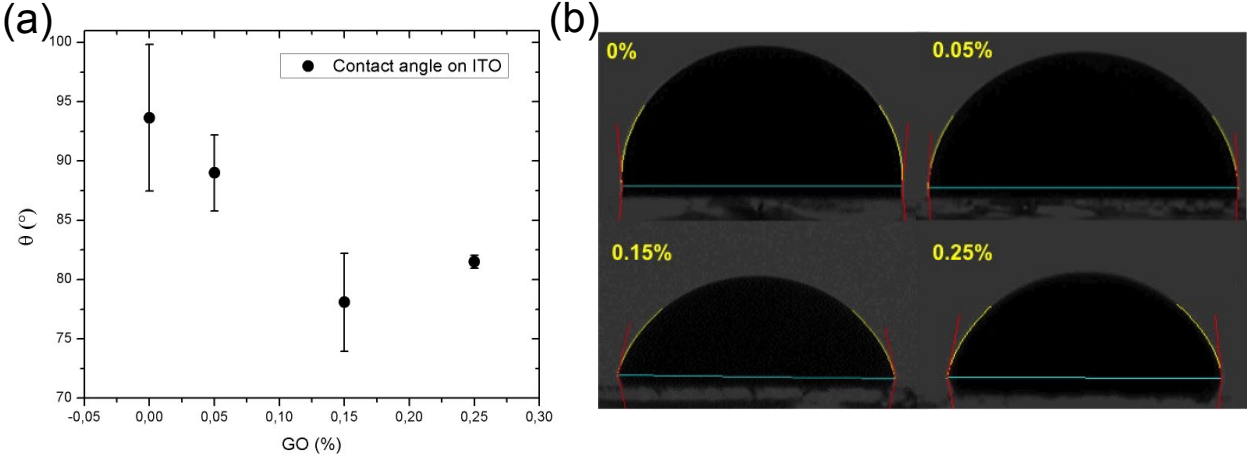


Figure 6. UV-vis absorption spectra of PEDOT:PSS compared with nanocomposites, spin-coated onto quartz glass substrates, after thermal annealing

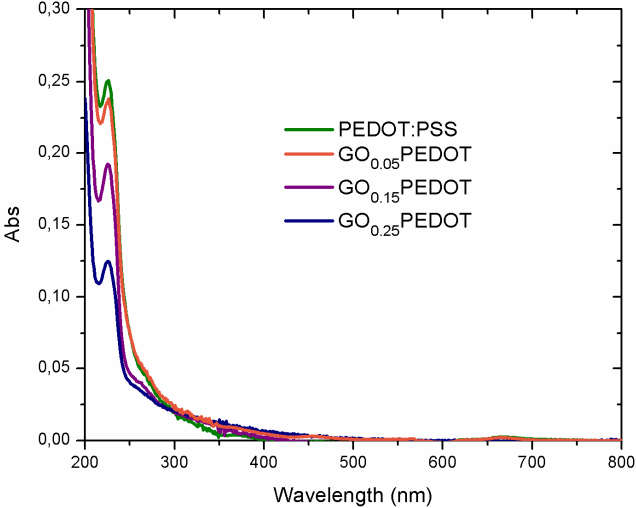


Table 1. GO/PEDOT:PSS concentration for the nanocomposites

Sample	GO/PEDOT:PSS concentration %wt/wt	GO/PEDOT:PSS Volume fraction
PEDOT:PSS	0	0
GO _{0.05} PEDOT	0.05	0.015
GO _{0.15} PEDOT	0.15	0.033
GO _{0.25} PEDOT	0.25	0.044

Table 2. Parameters of Cross Equation

Sample	η_0 (Pa*s)	η_∞ (Pa*s)	τ (s)	m
PEDOT:PSS	0.4	0.0040	5.80	1.85
GO _{0.05} PEDOT	5.0	0.0055	7.53	0.97
GO _{0.15} PEDOT	5.7	0.0090	11.37	0.90
GO _{0.25} PEDOT	9.0	0.0100	12.50	1.00

Table 3. Thermal analyses of PEDOT:PSS and nanocomposite films

Sample	Water loss step		PEDOT:PSS degradation step		
	H ₂ O loss %	Dehydration energy (kJ/mol)	Weight loss %	Onset point °C	Residue %
PEDOT:PSS	22.7	39.3	35.9	268	41.8
GO _{0.05} PEDOT	18.7	33.4	33.9	272	47.7
GO _{0.15} PEDOT	17.6	54.0	29.9	287	44.0
GO _{0.25} PEDOT	20.3	41.7	29.1	288	42.4